Cycle Detection and Characterization in Chemical Engineering

L. A. Briens and C. L. Briens
Dept. of Chemical and Biochemical Engineering, The University of Western Ontario, London, Ontario, Canada N6A 5B9

Nonperiodic cycles occur in times series obtained in many chemical engineering applications. Variations in the cycle characteristics provide valuable information about the system in which the time series was measured. New methods are developed to detect cycles and determine their characteristics such as the cycle time, its regularity, the cycle strength, and the regularity of the cycle amplitude. These methods are thoroughly validated with both mathematically generated and experimental time series. The best detection method for nonperiodic cycles uses either the V statistic or, if it fails, the new, more sensitive, but more complex, P statistic. Cycle characteristics can be used to detect flow regime transitions in multiphase systems such as risers, gas-solid, and gas-liquid-solid fluidized beds using signals from a variety of simple probes.

Introduction

A cycle can be defined as an interval over which certain phenomena are repeated. Cycles may be periodic or nonperiodic. With periodic cycles, the cycle time, which is the duration of one complete cycle, has a well defined and constant value. With nonperiodic cycles, the cycle time varies from one cycle to the next.

Cycles have been observed in nature and are usually nonperiodic. For example, there are cycles in the seasons, lunar and solar orbits, and animal and plant populations (Begon and Mortimer, 1986; Peters, 1994; Sanz, 1999). Diseases (Glass and Mackey, 1988; Mackey and Milton, 1987; West, 1990) and economic indicators (Peters, 1994, 1991) also exhibit cyclic variations.

Unit the work by Briens et al. (1999, 1997a,b,c,d), cycles had not been systematically identified and characterized in chemical engineering. They showed that time series in chemical engineering often exhibit cyclic behavior. The cycles are usually nonperiodic and variations in cycle time and cycle characteristics can provide valuable information about the system in which the times series was measured.

Several methods, reviewed below, have been proposed for the detection of nonperiodic cycles and the evaluation of their cycle time. No method, however, has been proposed to quantify other nonperiodic cycle characteristics such as the regularity and strength of the cyclic component.

Correspondence concerning this article should be addressed to C. L. Briens.

The objective of this article is therefore to develop new methods for the characterization of nonperiodic cycles. These methods and existing methods for cycle detection will be illustrated and validated with two mathematically generated time series and two experimental time series. Finally, the cycle detection and characterization methods will be applied to the identification of flow regimes in five different multiphase systems.

Time Series Used for Validation Tests

Validation tests were conducted with two mathematically generated times series and two experimental time series.

Mathematically generated time series

The advantage of the mathematically derived time series is that their parameters can be adjusted to change their characteristics. Two types of mathematically generated time series, which were sampled at 1 Hz with a total length of 30,000 s, were used in this study:

(1) *Sine Waves.* A sine wave is a cyclic, periodic time series. Figure 1a shows a sine wave with a period of 200 s.

(2) *Gaussian Cycle Time Sine Waves.* The period of each cycle is determined randomly from a Gaussian distribution. The Gaussian cycle time sine waves are therefore nonperiodic, as shown in Figure 1b.

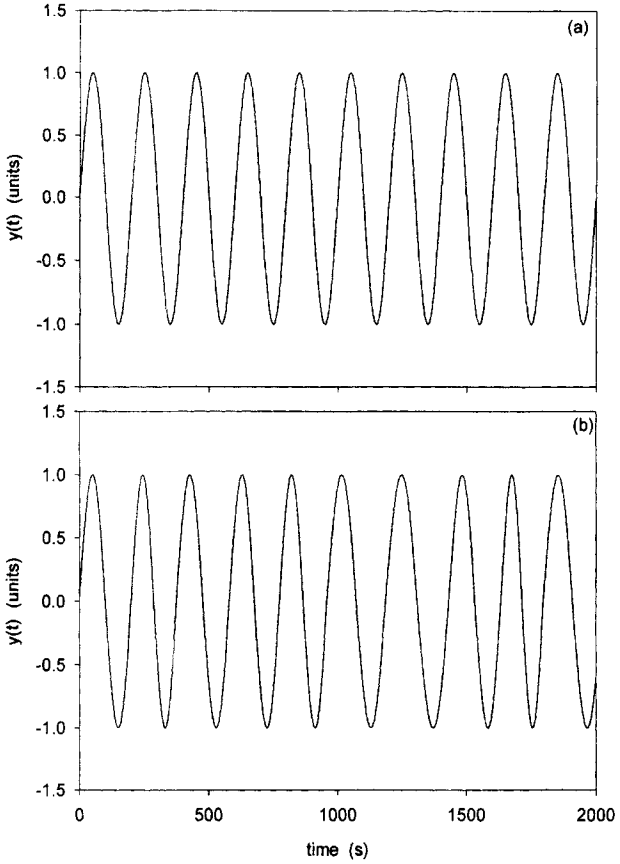

Figure 1. Segments of the mathematically generated time series.

(a) Sine wave (T = 200 s); (b) Gaussian cycle time sine wave (C_v = 0.15, T = 200 s).

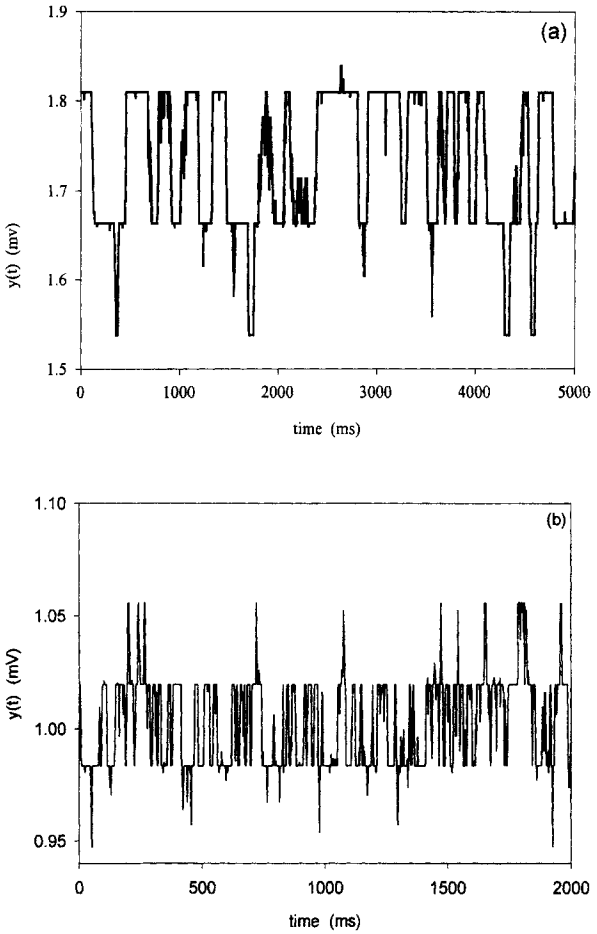

Figure 2. Segments of the experimental time series.

(a) Cross-sectional average conductivity; (b) bed pressure gradient fluctuations.

These two time series can be modified so the amplitude of each cycle is determined randomly from a Gaussian distribution.

Experimental time series

Two different time series were selected:

(1) Cross-Sectional Average Conductivity Time Series. The conductivity measurements were made in a gas-liquid-solid fluidized bed with diametrically opposed electrodes. The solids were 3 mm, 2,471 kg/m^3 glass beads, the superficial liquid velocity was 4 cm/s, and the superficial gas velocity was 6 cm/s. Experimental details may be found in Briens (2000) and Briens et al. (1997b). The time series length was 60 s with a sampling frequency of 500 Hz. This time series is cyclic, but very nonperiodic (Figure 2a). Figure 2a shows that the signal appeared to be a combination of nearly constant intervals interspersed with rapidly changing sections which are believed to result from the passage of gas bubbles.

(2) Bed Pressure Gradient Time Series. The pressure gradient measurements were made in a gas-liquid-solid fluidized bed. The solids were 2.1 mm, 1,290 kg/m^3 polypropylene particles, the superficial liquid velocity was 2.45, cm/s, and the superficial gas velocity was 1.7 cm/s. Experimental details may be found in Briens (2000) and Briens et al. (1997c). The time series length was 60 s with a sampling frequency of 500 Hz. Figure 2b shows that this time series is cyclic, but very nonperiodic, and is similar in appearance to the conductivity time series shown in Figure 2a.

Cycle Detection Methods

This section reviews and tests four previously published cycle detection methods: the power spectra, the crossing frequency, Hurst analysis, and the V statistic. It also introduces a new method: the P statistic.

Power spectrum

The spectral density of a time series can be obtained from the product of its Fourier transform by its complex conjugate. The power spectrum is the plot of the spectral density against time or frequency.

Figure 3 shows the power spectra of the sine wave, Gaussian cycle time sine wave, and the cross-sectional average conductivity time series. These results were obtained with Hann windowing (similar results were obtained with Bartlett and Welch windows). Only the periodic cycle of 200 s of the sine wave time series can be clearly identified (Figure 3a). A dominant period of about 200 s can be identified for the Gaussian cycle time sine wave, but it is not as clear (Figure 3b). A cycle

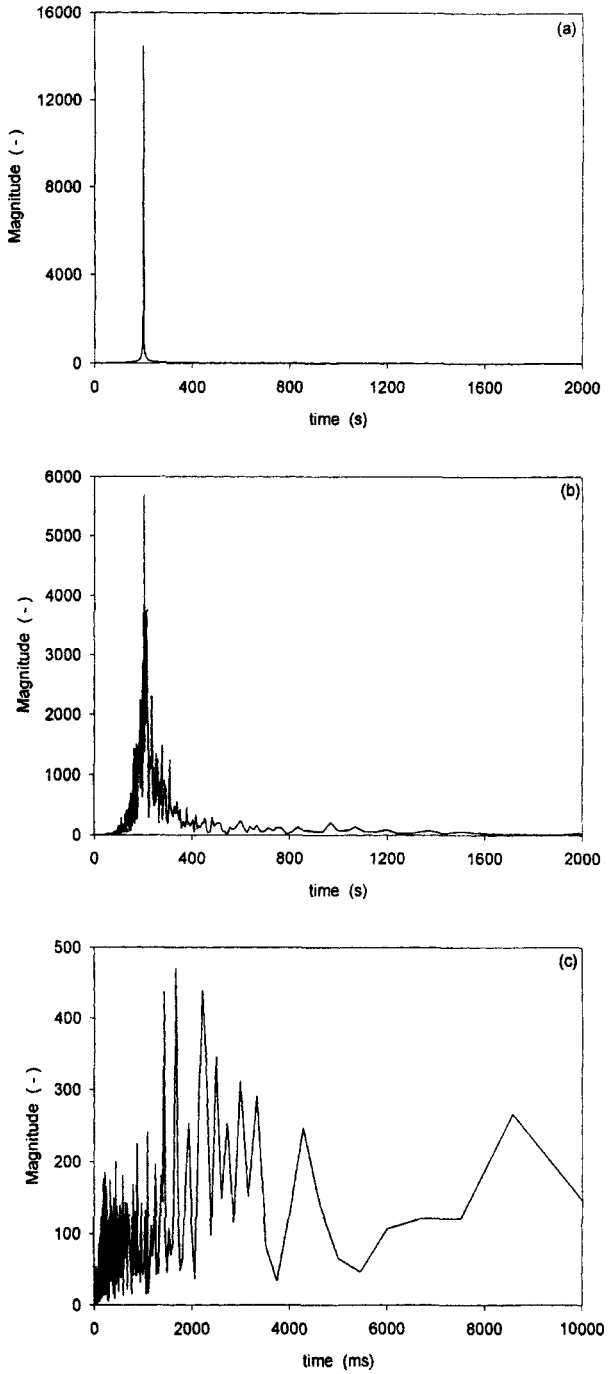

Figure 3. Power spectra of various time series.

(a) Sine wave (T = 200 s); (b) Gaussian cycle time sine wave (C_v = 0.15, T = 200 s); (c) cross-sectional average conductivity.

time cannot be identified for the cross-sectional average conductivity time series (Figure 3c). The power spectra can therefore only identify cycle times of periodic or nearly periodic time series.

In theory, an average cycle time can be calculated from the power spectrum. However, the calculated value would be very sensitive to the "tail" of the spectrum: for the cross-sectional average conductivity time series, stopping the integration at 10,000 ms gives an average cycle time of 251 ms while stopping at 2,000 ms gives 175 ms.

Crossing frequency

The crossing frequency can theoretically provide the cycle time of a nonperiodic time series (Briens, 2000; vander Stappen, 1996). It is obtained by counting the number of times the signal crosses its average line.

The crossing frequency method gave good results with the mathematical functions, but failed with the experimental time series. With the experimental time series, high frequency fluctuations caused the signal to repeatedly cross the average line. The crossing frequency would require extensive frequency filtering which might distort the frequencies of interest.

Hurst analysis

Hurst developed a method to quantify the persistence of time series (Hurst, 1951). It divides the time series in time intervals of length τ. A rescaled range is calculated for each interval. The average of the rescaled ranges $(R/S)_\tau$ can then be obtained for all the intervals of length τ. Changing the value of the interval length τ and plotting $\ln(R/S)_\tau$ as a function of $\ln(\tau)$ gives a curve whose slope is the Hurst exponent H.

According to Peters (1994), if the time series exhibits cyclic behavior, the Hurst exponent H changes at certain values of the interval length τ and the plot of $\ln(R/S)_\tau$ vs. $\ln(\tau)$ is not a straight line. The break in this plot corresponds to the cycle time. Figure 4 shows how the cycle time can be obtained with the Hurst method. With the sine wave and the Gaussian cyclé time sine wave (Figures 4a and 4b), the break occurs around 200 s. With the cross-sectional average conductivity time series (Figure 4c), the break is not clear and an approximate value of about 250 ms can be obtained for the cycle time.

A problem with using Hurst's rescaled range analysis to detect cycles is that it is difficult to determine the exact location of the break in the $\ln(R/S)_\tau$ vs. $\ln(\tau)$ plots. For example, there may be fluctuations due to harmonics for periodic or nearly periodic time series (Figures 4a and 4b); the cycle time corresponds to the location where the harmonics begin. Also, the Hurst exponent H may change very gradually (Figure 4c).

Although the Hurst method may not always give accurate results, it can tolerate minor changes in the calibration constants of the measuring equipment. Adding a constant value to a single or multiplying it by a constant value does not change the value of the Hurst exponent.

V statistic

Peters (1994) introduced the V statistic to detect cyclic behavior in the stock markets

$$V_\tau = \frac{(R/S)_\tau}{\sqrt{\tau}} \tag{1}$$

The V statistic transforms a break in the $\ln(R/S)_\tau$ vs. $\ln(\tau)$ curve into a more easily detectable peak if the break is between a section of slope H larger than 0.5 and a section of a slope smaller than 0.5. Since it is based on Hurst analysis, it

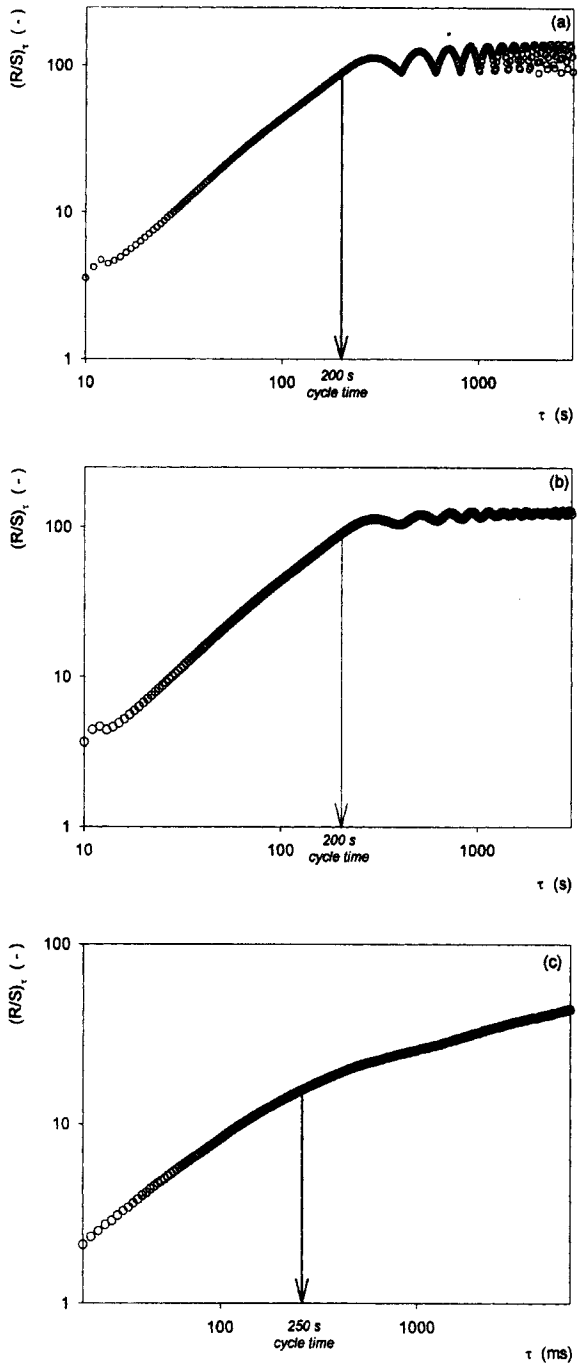

Figure 4. Log-log plots of $(R/S)_\tau$ vs. for various time series.

(a) Sine wave (T = 200 s); (b) Gaussian cycle time sine wave (C_v = 0.15, T = 200 s); (c) cross-sectional average conductivity.

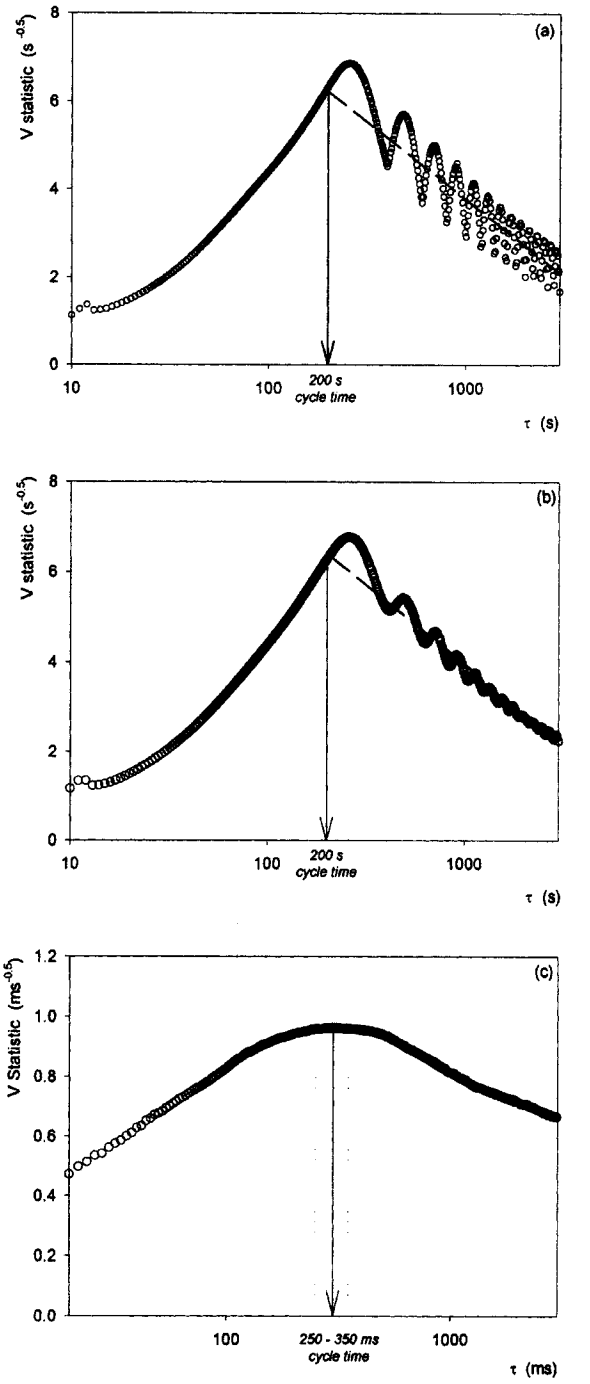

Figure 5. V statistic plots for various time series.

(a) Sine wave (T = 200 s); (b) Gaussian cycle time sine wave (C_v = 0.15, T = 200 s); (c) cross-sectional average conductivity.

can also tolerate changes in calibration constants of the measuring equipment.

Figure 5 shows how much easier the detection of the cycle time becomes with the V statistic. With the sine wave (Figure 5a) and the Gaussian cycle time sine wave (Figure 5b), the cycle time is 200 s. With the cross-sectional average conductivity time series (Figure 5c), the V statistic shows a well-defined peak. The peak width, however, is broad with a cycle time ranging between 250 and 350 ms. This indicates that the change in the Hurst exponent H is not abrupt: the signal is cyclic but not periodic.

P statistic

In some cases, the V statistic does not exhibit a peak. Figure 6 shows such an example which was obtained with the bed pressure gradient time series. This could mean there is

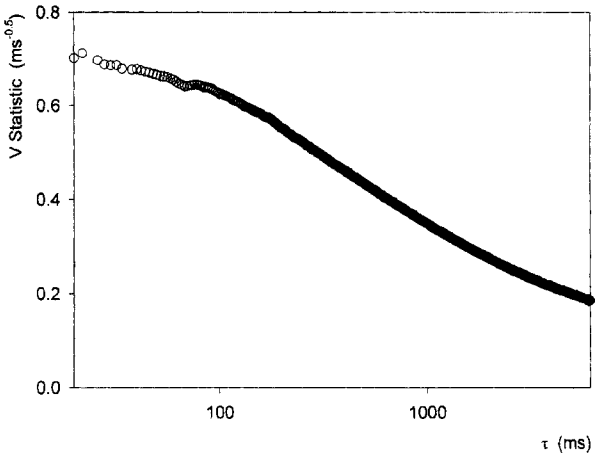

Figure 6. *V* statistic for the bed pressure gradient time series.

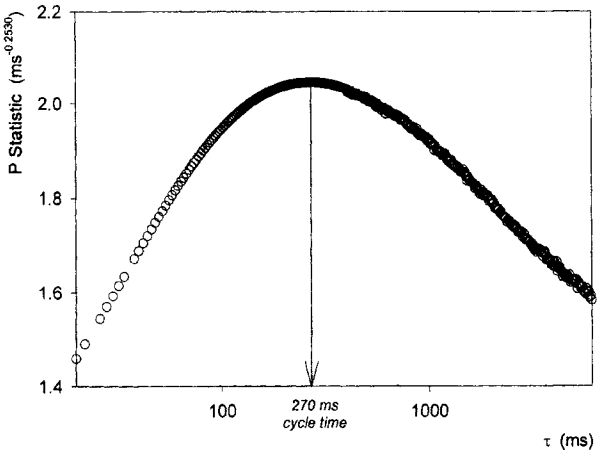

Figure 7. *P* statistic for the bed pressure gradient time series.

no cycle in the signal. Alternately, it could mean the time series is cyclic and that the break in the $\ln(R/S)_\tau$ vs. $\ln(\tau)$ plot occurs without the slope switching from a section where it is smaller than 0.5 to a section where it is larger than 0.5.

A P statistic was therefore introduced to generalize the V statistic to detect any break in the $\ln(R/S)_\tau$ vs. $\ln(\tau)$ plot. It is defined as (Briens, 2000)

$$P_\tau = \frac{(R/S)_\tau}{\tau^\gamma} \tag{2}$$

where γ is an exponent between 0 and 1. The P statistic is equivalent to the V statistic when γ equals 0.5. As for the V statistic, the P statistic can tolerate changes in calibration constants of the measuring equipment.

Several empirical methods were tested to select the most appropriate value of γ. The best method selects the value of γ which maximizes the ratio (Briens, 2000)

$$\frac{\text{maximum } P \text{ statistic} - \text{maximum of } P \text{ statistics at the minimum and maximum } \tau}{\text{maximum of } P \text{ statistics at the minimum and maximum } \tau}$$

Figure 7 shows that the P statistic clearly identifies the cyclic behavior of the bed pressure gradient time series. The optimized value of exponent γ was 0.253. The P statistic can identify cyclic behavior when the V statistic fails.

Conclusions

The power spectrum can only identify periodic or nearly periodic cycles. The crossing frequency method works well for the mathematically generated signals, but is too sensitive to noise and completely fails with the experimental time series. Hurst's analysis identifies cycles but cannot easily provide accurate cycle times. The V statistic is easy to use and provided a clear cycle time for three of the four example time series. The new P statistic successfully identifies cycles and provides a cycle time when the V statistic fails.

Cycle Characterization Methods

The previous section showed how to detect cycles and determine the cycle time. This section develops and tests new criteria to quantify other important properties of a cycle. A periodic time series such as a sine wave has a single constant cycle time and amplitude. A nonperiodic cyclic time series, however, does not have a single cycle time or amplitude, but a distribution of cycle times and amplitudes. The regularity characterizes the width of this distribution. Since it is often impossible to identify individual cycles in the time series, special methods are developed to quantify the regularity of the cycle time and of the amplitude. A method is also derived to estimate the strength of the cycles.

The cycle characterization methods developed for this study are not intended to be universal characteristics which could be used to compare completely different signals, such as measurements from completely different reactors. Their purpose is to quantify the evolution of time series from a given type of sensor in a multiphase reactor as conditions such as position, phase velocities, or properties vary.

Regularity of the cycle time

If the V statistic successfully identified the cycle, the regularity of the cycle time can be characterized with (Briens, 2000)

$$R_T = \frac{V_T \Delta t}{\sqrt{T}} \tag{3}$$

where Δt is the sampling interval, T is the average cycle time, and V_T is the value of the V statistic which corresponds to T.

If the V statistic failed, the regularity of the cycle time can be obtained from the P statistic

$$R_T = \frac{P_T \Delta t}{T^{(1-\gamma)}} \tag{4}$$

where P_T is the value of the P statistic which corresponds to the cycle time T.

The regularity R_T of the cycle time has the following attractive properties:

- It is dimensionless.
- It is independent of the cycle time. This can be theoretically demonstrated for the sine wave. This was also verified for the Gaussian cycle time sine wave (Briens, 2000).
- It is independent of the sampling interval Δt. This can be theoretically demonstrated for the sine wave. This was verified for the Gaussian cycle time sine wave and the experimental time series (Briens, 2000). This, however, assumes that the sampling frequency provides enough points to define accurately the shape of every cycle.
- It is independent of the cycle amplitude. This results directly from the fact that the calculated rescaled range $(R/S)_\tau$ is not affected by the addition of a constant value or by a change in the amplitude of the cycle component.
- It is independent of the regularity of the cycle amplitude. This can be tested by modifying the mathematically generated time series so that the amplitude of each cycle is determined randomly from a Gaussian distribution. It was thus shown that the regularity of the cycle amplitude does not affect the calculated regularity of the cycle time (Briens, 2000).
- It accurately quantifies the regularity of the cycle time. Figure 8 shows that the calculated cycle time regularity R_T decreases regularly as the mathematically generated time series are made less regular by increasing the coefficient of variation of the cycle time.

Regularity of the cycle amplitude

The regularity of the cycle amplitude can be calculated with the following procedure (Briens, 2000):

(1) Start at a point determined randomly. Divide the time series into N_s segments of length T, where T is the cycle time determined with either the V or the P statistic.

(2) Calculate the range of each segment by taking the difference between the maximum and minimum values.

(3) Repeat steps 1 and 2. The number of repeats is n_r.

(4) Calculate the average m_R and standard deviation σ_R of the $(n_r \times N_s)$ range values.

(5) Calculate the regularity of the cycle amplitude

$$R_A = 1 - \frac{\sigma_R}{m_R} \tag{5}$$

Note that R_A may assume a negative value.

The regularity R_A of the cycle amplitude has the following attractive properties:

- It is dimensionless.
- It is independently of the cycle time. This was verified for the sine and Gaussian cycle time sine waves (Briens, 2000).
- It is independent of the regularity R_T of the cycle time. This was verified for the Gaussian cycle time sine wave (Briens, 2000).
- It is independent of the sampling interval Δt. This was verified for the sine and Gaussian cycle time sine waves (Briens, 2000).
- It is independent of the cycle amplitude. This was verified for the sine and Gaussian cycle time sine wave (Briens, 2000).
- It accurately quantifies the regularity of the cycle amplitude. Figure 9 shows that the calculated cycle amplitude regularity R_A decreases regularly as the mathematically generated time series are made less regular by increasing the coefficient of variation of the cycle amplitude.

Cycle strength

The cycle strength A can be calculated with the following procedure (Briens, 2000):

(1) Divide the time series into N_s segments of length T, where T is the cycle time determined with either the V or the P statistic. Start at a point determined randomly.

(2) For each segment, calculate the average value of the signal, its standard deviation, and the difference a_s between the standard deviation and the average.

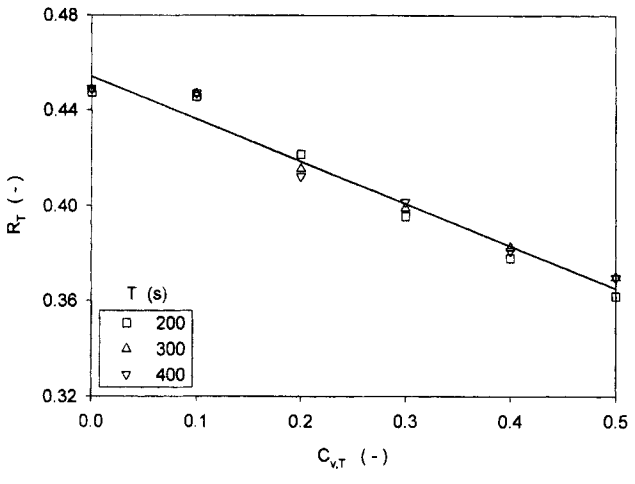

Figure 8. Effect of imposed irregularity in the cycle time of mathematically generated time series on calculated cycle time regularity R_T.

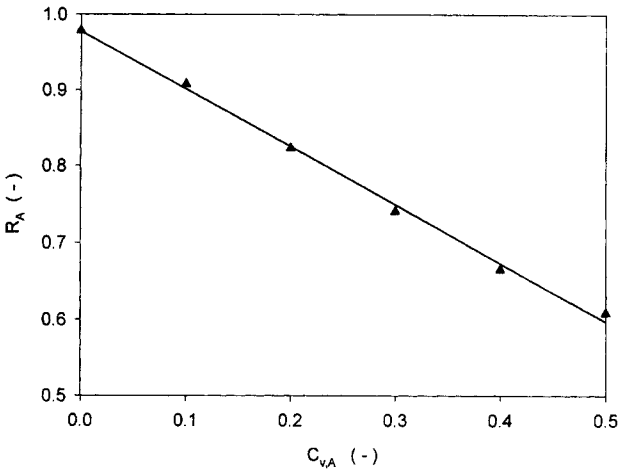

Figure 9. Effect of imposed irregularity in the cycle amplitude of mathematically generated time series on calculated cycle amplitude regularity R_A.

(3) Repeat steps 1 and 2. The number of repeats is n_r.

(4) Calculate the average A of the $(n_r \times N_s)$ values of a_s. This average represents the cycle strength.

The cycle strength has the following attractive properties:

- It is independent of the cycle time. This was verified for the sine and Gaussian cycle time sine waves (Briens, 2000).
- It is independent of the sampling interval Δt. This was verified for the sine and Gaussian cycle time sine waves (Briens, 2000).
- It is independent of the regularity of the cycle time. This was verified for the sine and Gaussian cycle time sine waves (Briens, 2000).
- It accurately quantifies the cycle strength. This was verified in two ways. First, if a constant value α is added to a cyclic time series, the strength of the cyclic component should decrease. This was theoretically verified for the sine wave and empirically for the Gaussian cycle time sine wave (Briens, 2000) (Figure 10a). Second, if a cyclic time series is multiplied by a constant value α, the strength of the cyclic component should increase. This was verified theoretically for the sine wave and empirically for the Gaussian cycle time sine wave (Briens, 2000) (Figure 10b).

Detection of Flow Regimes

Most multiphase systems exhibit different flow regimes which depend on fluid velocities and the properties of the particles and fluids. The performance of a multiphase system greatly depends on its flow regime. It is therefore essential to detect the flow regime in which a particular system is operating. This is especially important in systems where particle or fluid properties evolve.

The purpose of this section is to apply the cycle analysis tools developed above to detect flow regime transitions in five different multiphase systems, using a variety of simple probes. Cycle analysis characterizes signal fluctuations and can thus extract useful information from probe signals.

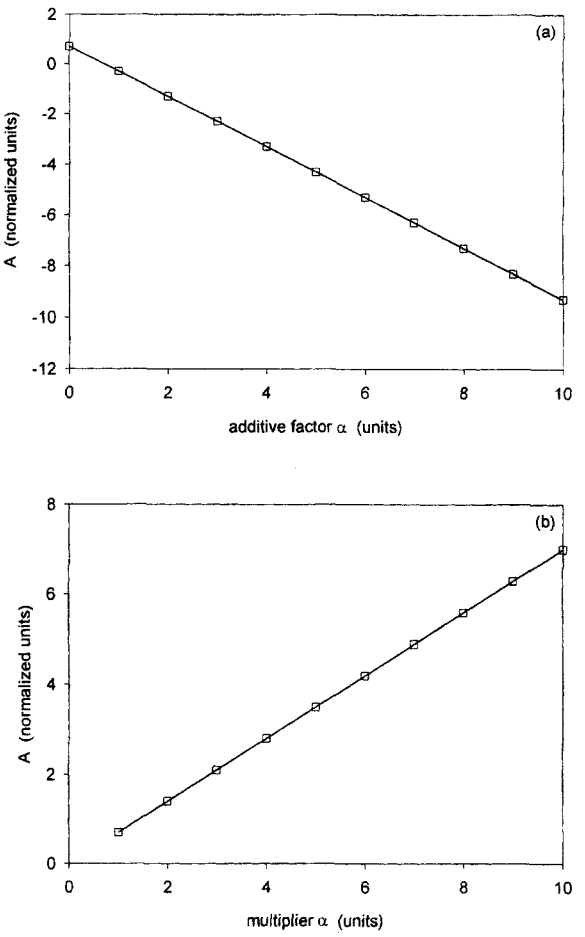

Figure 10. Effect of (a) adding value α and (b) multiplying value α of the original time series in the cycle strength of the Gaussian cycle time sine waves ($C_v = 0.15$, $T = 200$ s).

Flow regimes in a three-phase bed of glass beads

The conductivity measurements were made in a 0.10 m diameter gas-liquid-solid fluidized bed. The conductivity measurements were performed with the tips of two rods on the column axis and at 31 and 36 cm above the grid. The solids were 3 mm, 2,471 kg/m^3 spherical glass beads, the liquid was a 1 wt. % aqueous solution of Na_2HPO_4, and the gas was oil-free air. The time series length was 60 s with a sampling frequency of 500 Hz. Experimental details may be found in Briens (2000) and Briens et al. (1997b). The superficial gas velocity was 6 cm/s. A thorough analysis, using accurate conductivity and pressure measurements with careful calibration, indicated that there were two flow regime transitions: from the fixed bed to the agitated bed U_{Lma} and then from the agitated to the fluidized bed U_{Lmf} at superficial liquid velocities of about 1 cm/s and 2 cm/s, respectively (Briens, 2000; Briens et al., 1997b).

Figure 11 shows the results of cycle analysis as a function of the liquid superficial velocity. The cycle time regularity R_T, the amplitude regularity R_A, and the cycle strength A allow clear detection of the minimum fluidization liquid velocity U_{Lmf}. The cycle strength is the most suitable for process control since adjusting the superficial liquid velocity to get a cycle strength smaller than -0.45 mV would maintain fluidization. The minimum agitation velocity U_{Lma}, at the transition from the fixed bed to the agitated bed regime can be clearly detected from the cycle amplitude regularity R_A.

In the fixed bed, conductivity fluctuations can only result from gas bubbles. The fraction of these fluctuations which is cyclic decreases when the superficial liquid velocity is increased although the standard deviation of the raw signal increases. This means that the cyclic fraction of the signal becomes smaller as the velocity is increased: bubbling becomes more random.

In the fluidized bed, the strength of the cyclic fraction of the conductivity fluctuations decreases even more sharply when the superficial liquid velocity is increased, although the standard deviation of the raw signal remains approximately constant. The cyclic fraction of the signal becomes even smaller and less regular in both time and amplitude. This results from the random-like motion of the particles, which contributes to the conductivity fluctuations.

Flow regimes in a three-phase bed of low density particles

The equipment was the same as for the three-phase bed of glass beads. The particles were polypropylene with a density

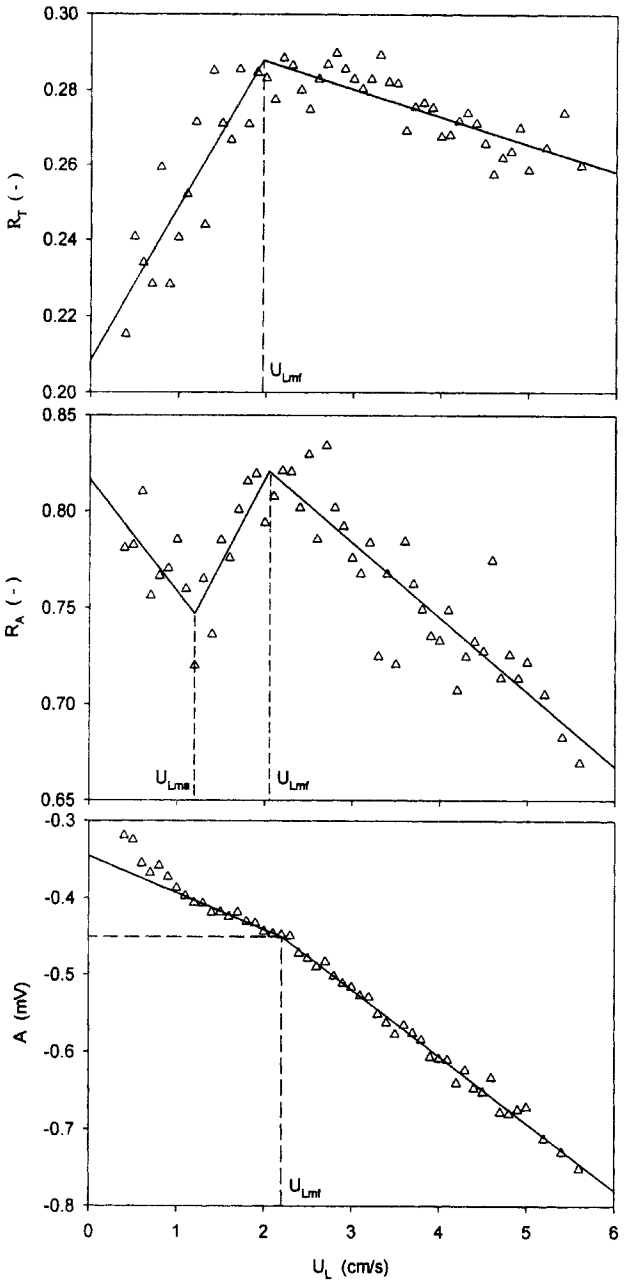

Figure 11. Transitions in a three-phase fluidized bed of glass beads.

Local conductivity measurements.

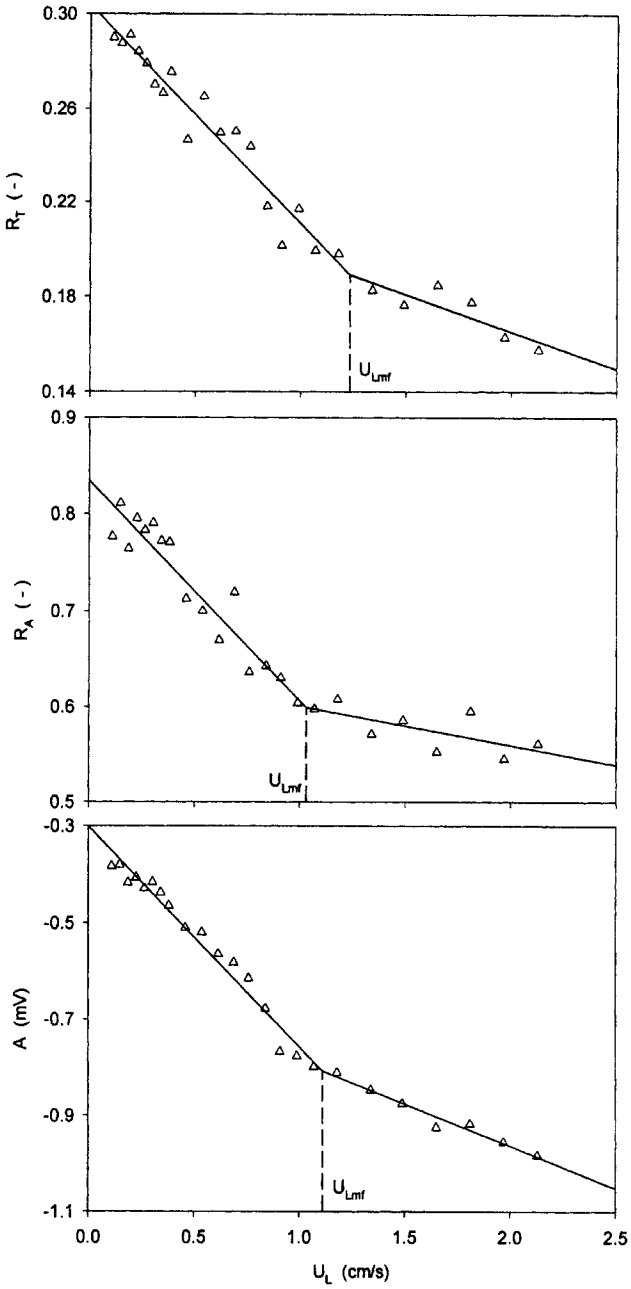

Figure 12. Transitions in a three-phase fluidized bed of polypropylene particles.

Local conductivity measurements.

of 1,290 kg/m^3, a volume-equivalent diameter of 2.1 mm, and a sphericity of 0.82. Experimental details may be found in Briens (2000) and Briens et al. (1997c). The superficial gas velocity was 3 cm/s. The transition to the fluidized-bed regime, which was not as sharp as with the glass beads, occurred at a superficial liquid velocity of about 1 cm/s.

Figure 12 shows that the cycle time regularity R_T, the amplitude regularity R_A, and the cycle strength A allow clear detection of the minimum fluidization liquid velocity U_{Lmf}. There is a slight variation of the transition velocity, going from 1.03 cm/s with the amplitude regularity to 1.23 cm/s with the cycle time regularity. This confirms the visual observations of a gradual transition from fixed to fluidized bed. All three indices would be suitable for process control: fluidization can be maintained by setting the cycle time regularity below 0.8, the amplitude regularity below 0.58, and the cycle strength below 0.85 mV.

Core-annulus structure in a pilot-plant riser

Experiments were conducted in a pilot-plant riser, 18 cm in diameter, with FCC catalyst, a solids flux of 300 kg/(s·m^2), and a superficial gas velocity of 6.3 m/s. Measurements were conducted at various radial locations with an optical fiber

probe with 2,000 Hz sampling frequency. More details are provided in Briens (2000). The riser was operating with a core-annulus structure. There was a clear transition to the dense-phase annulus at a dimensionless radius r/R of 0.65. The transition to the dilute core was not as sharp, with a wide intermediate zone.

Figure 13 shows that the cycle time regularity R_T, the amplitude regularity R_A, and the cycle strength A provide clear detection of the transition between the annulus and the intermediate zone. The cycle amplitude regularity R_A can also discriminate between the intermediate region and the dilute core.

The cyclic variation of the local solids concentration measured with the optical fiber probe is believed to originate with waves at the annulus surface. The effect of the surface waves becomes less pronounced as the probe is pushed deeper into the annulus and the cycle strength A thus becomes gradually smaller.

Core-annulus structure in an industrial riser

Experiments were conducted in the 1 m diameter riser of an industrial fluid catalytic cracker under typical industrial conditions. Measurements were conducted at various radial locations with a momentum probe with 200 Hz sampling frequency. More details are provided in Briens (2000). The riser

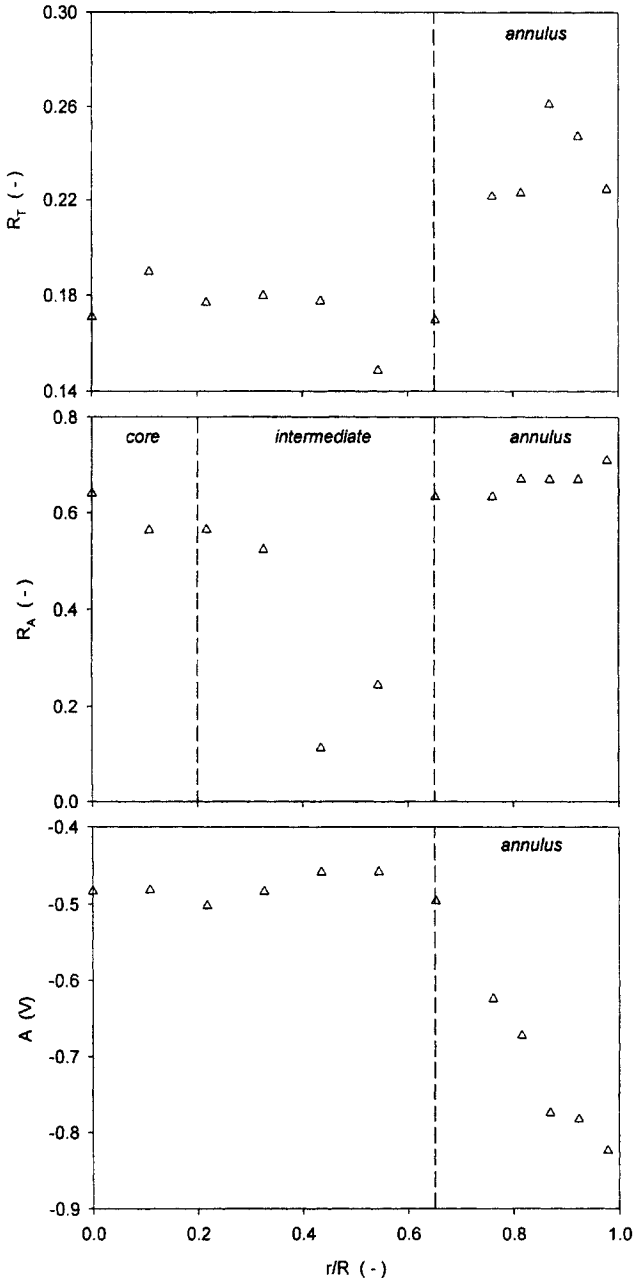

Figure 13. Transitions in a pilot-plant riser.
Optical fiber measurements.

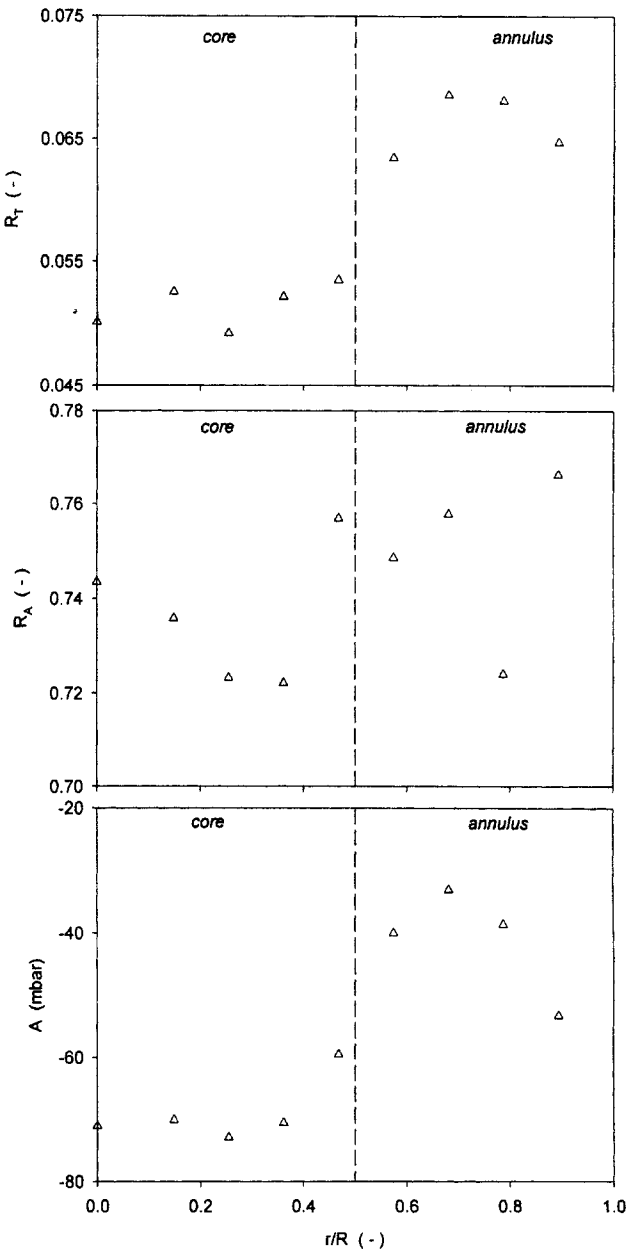

Figure 14. Transitions in an industrial riser.
Momentum probe measurements.

was operating with a core-annulus structure. It was difficult to determine exactly the extent of the intermediate zone since there were not as many measurement points within that zone; it was approximately between dimensionless radial positions of 0.4 and 0.6. The transition between core and annulus can therefore be set at a dimensionless radial position of about 0.5.

Figure 14 shows that the cycle time regularity R_T, the amplitude regularity R_A, and the cycle strength A detect the transition between the annulus and the core. The cyclic variation of the local solids momentum is believed to originate with waves at the annulus surface. As in the pilot-plant riser (Figure 13), the effect of the surface waves becomes less pronounced as the probe is pushed deeper into the annulus and the cycle strength A thus becomes gradually smaller (Figure 14).

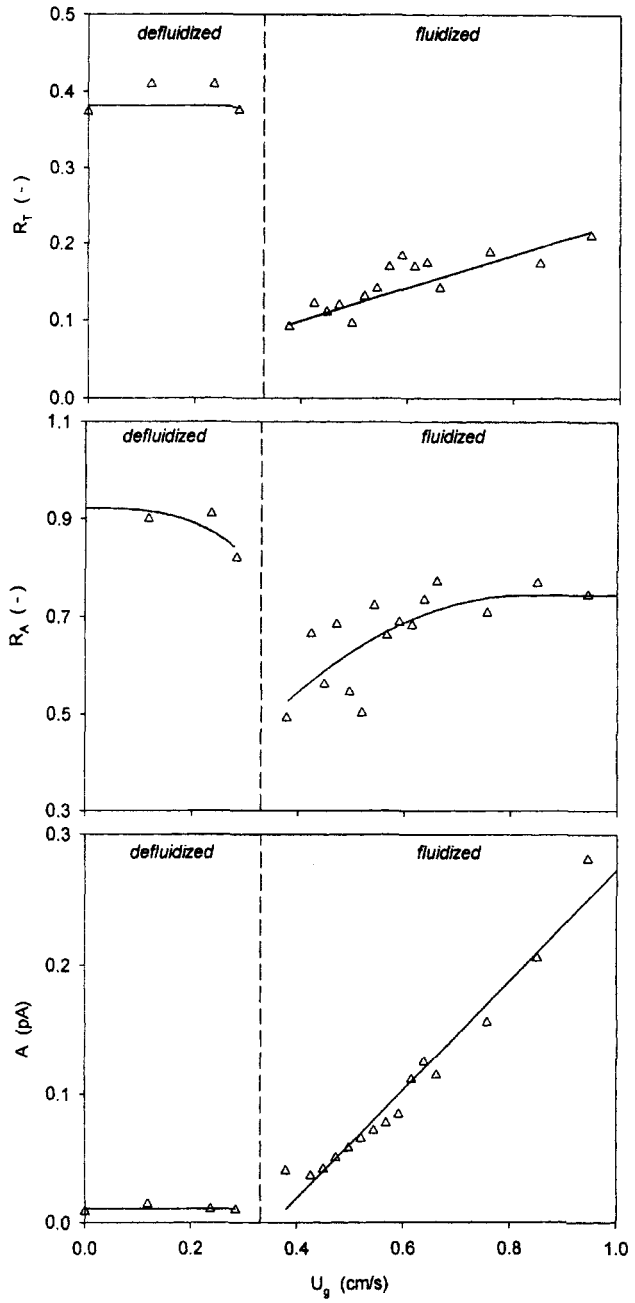

Figure 15. Transitions in a gas-solid fluidized bed.
Triboelectric probe measurements.

Defluidized zones in a gas-solid fluidized bed

Experiments were conducted in a 50 cm square column with PVC polymer particles, a group A powder according to Geldart's classification, which were fluidized with nitrogen. A probe within the bed measured the triboelectric current generated by the friction of the bed particles on its surface. Its signal was sampled at a 800 Hz frequency. The minimum fluidization velocity was about 0.33 cm/s (Briens, 2000; Briens et al., 1999).

Figure 15 shows that the cycle time regularity R_T, the cycle amplitude regularity R_A, and the cycle strength A detect the transition from fixed to fluidized bed. The cycle time regularity R_T, the cycle strength A, and the amplitude regularity R_A all steadily increase as the superificial gas velocity is further increased and the friction of the particles on the probe becomes more intense and regular. Although the cycle strength is very small in the defluidized bed, the cycle time and amplitude regularities are very high. The triboelectric current, which should have been zero in the defluidized bed, was contaminated by highly regular 50 Hz noise from the mains. This can be confirmed from the measured cycle time which is 20 ms in the defluidized bed and about 500 ms in the fluidized bed (Briens, 2000; Briens et al., 1999).

Similar results were obtained with other polymers and in an industrial bed (Briens, 2000; Briens et al., 1999).

Conclusions

The best detection method for nonperiodic cycles uses a combination of the V and P statistics. If the V statistic fails to detect cyclic behavior, the new, more sensitive P statistic should be used. Accurate cycle times can thus be obtained.

New parameters characterize the strength of the cyclic component and the regularities of the cycle time and amplitude.

Cycle characteristics can be used to detect flow regime transitions in multiphase systems such as risers, gas-solid, and gas-liquid-solid fluidized beds using signals from a variety of simple probes.

Acknowledgments

The authors gratefully acknowledge the Natural Sciences and Engineering Research Council (NSERC) of Canada for their financial support (postgraduate scholarship) to L. A. Briens and an operating grant to C. L. Briens. The authors would also like to thank E. Barthel, J. R. Bernard, J. Bousquet, J. M. Le Blévec, D. Nevicato, and A. Tedoldi from TOTALFINAELF for helping us test new concepts under realistic conditions.

Notation

a_s = difference between standard deviation and average, units of original time series
A = cycle strength, units of original time series
$C_{v,A}$ = coefficient of variation of the cycle amplitude
$C_{v,T}$ = coefficient of variation of the cycle time
m_R = average of the range values, units of original time series

n_r = number of times a calculation is repeated
N_s = number of segments used for the calculation of R_A and A
P_τ = P statistic corresponding to a subperiod length of τ, $s^{-\gamma}$
R_A = regularity of the cycle amplitude
R_T = regularity of the cycle time
$(R/S)_\tau$ = rescaled range for the subperiod of length τ
T = cycle time, s
V_T = V statistic corresponding to the cycle time T, $s^{-0.5}$
V_τ = V statistic corresponding to a subperiod length of τ, $s^{-0.5}$
Δt = time interval between successive data points acquired by the data acquisition system, s
γ = exponent for the P statistic
σ_R = standard deviation of the range values, units of the original time series
τ = length of the subperiod, s

Literature Cited

Begon, M., and M. Mortimer, *Population Ecology. A Unified Study of Plants and Animals*, Blackwell Scientific Publications, Palo Alto, CA (1986).

Briens, L. A., "Identification of Flow Regimes in Multiphase Reactors by Time Series Analysis," PhD Thesis, Univ. of Western Ontario, London, Canada (2000).

Briens, C. L., L. A. Briens, E. Barthel, J. M. Le Blévec, A. Tedoldi, and A. Margaritis, "Detection of Local Fluidization Characteristics Using the V Statistic," *Power Tech.*, **102**, 95 (1999).

Briens, C. L., L. A. Briens, J. Hay, C. Hudson, and A. Margaritis, "Hurst's Analysis to Detect Minimum Fluidization and Gas Maldistribution in Fluidized Beds," *AIChE J.*, **43**, 1904 (1997a).

Briens, L. A., C. L. Briens, A. Margaritis, and J. Hay, "Minimum Liquid Fluidization Velocity in Gas-Liquid Fluidization Beds," *AIChE J.*, **43**, 1180 (1997b).

Briens, L. A., C. L. Briens, A. Margaritis, and J. Hay, "Minimum Liquid Fluidization Velocity in Gas-Liquid-Solid Fluidized Beds of Low Density Particles," *Chem. Eng. Sci.*, **52**, 4231 (1997c).

Briens, C. L., C. Mirgain, M. Del Pozo, R. Loutaty, and M. A. Bergougnou, "Evaluation of a Gas-Solids Mixing Chamber with an Annular Solids Jet Through Cross-Correlation and Hurst's Analysis," *AIChE J.*, **43**, 1469 (1997d).

Glass, L., and M. C. Mackey, *From Clocks to Chaos. The Rhythms of Life*, Princeton University Press, Princeton, NJ (1988).

Hurst, H. E., "Methods of Using Long-Term Storage in Reservoirs," *ASCE*, **116**, 770 (1951).

Mackey, M. C., and J. C. Milton, "Dynamical Diseases," *Annals New York Acad. Sci.*, **504**, 16 (1987).

Peters, E. E., *Fractal Market Analysis. Applying Chaos Theory to Investment Economics*, Wiley, New York (1994).

Peters, E. E., *Chaos and Order in the Capital Markets*, Wiley, New York (1991).

Sanz, C., "Summer of Danger," *Discover*, **20**, 64 (1999).

Vander Stappen, M. L. M., "Chaotic Hydrodynamics of Fluidized Beds," PhD Thesis, Delft Univ., Netherlands (1996).

West, B. J., *Fractal Physiology and Chaos in Medicine. Studies of Nonlinear Phenomena in Life Science. Vol. 1*, World Scientific Co. Pte. Ltd., Singapore (1990).

Manuscript received Nov. 22, 2000.